

Flight Control of TUAV with Coaxial Rotor and Ducted Fan Configuration by NARMA-L2 Controllers for Enhanced Situational Awareness

Igor Astrov, Andrus Pedai, and Boris Gordon

Abstract—This paper focuses on a critical component of the situational awareness (SA), the control of autonomous vertical flight for tactical unmanned aerial vehicle (TUAV). With the SA strategy, we proposed a two stage flight control procedure using two autonomous control subsystems to address the dynamics variation and performance requirement difference in initial and final stages of flight trajectory for an unmanned helicopter model with coaxial rotor and ducted fan configuration. This control strategy for chosen model of TUAV has been verified by simulation of hovering maneuvers using software package Simulink and demonstrated good performance for fast stabilization of engines in hovering, consequently, fast SA with economy in energy can be asserted during search-and-rescue operations.

Keywords—Coaxial rotors, ducted fan, NARMA-L2 neurocontroller, situational awareness, tactical unmanned aerial vehicle.

I. INTRODUCTION

SITUATION awareness has been formally defined as “the perception of elements in the environment within a volume of time and space, the comprehension of their meaning, and the projection of their status in the near future” [1]. As the term implies, situation awareness refers to awareness of the situation. Grammatically, situational awareness (SA) refers to awareness that only happens sometimes in certain situations.

SA has been recognized as a critical, yet often elusive, foundation for successful decision-making across a broad range of complex and dynamic systems, including emergency response and military command and control operations [2].

The term SA have become commonplace for the doctrine and tactics, and techniques in the U.S. Army [3]. SA is defined as “the ability to maintain a constant, clear mental picture of relevant information and the tactical situation including friendly and threat situations as well as terrain”. SA allows

leaders to avoid surprise, make rapid decisions, and choose when and where to conduct engagements, and achieve decisive outcomes.

The tactical unmanned aerial vehicle (TUAV) is one of the key tools to gather the information to build SA for all leaders. The TUAV is the ground maneuver commander's primary day and night system. The TUAV provides the commander with a number of capabilities including:

- Enhanced SA.
- Target acquisition.
- Battle damage assessment.
- Enhanced battle management capabilities (friendly situation and battlefield visualization).

The combination of these benefits contributes to the commander's dominant SA allowing him to shape the battlefield to ensure mission success and to maneuver to points of positional advantage with speed and precision to conduct decisive operations. Some conditions for conducting aerial reconnaissance with TUAVs are as follows.

- Time is limited or information is required quickly.
- Detailed reconnaissance is not required.
- Extended duration surveillance is not required.
- Target is at extended range.
- Threat conditions are known; also the risk to ground assets is high.
- Verification of a target is needed.
- Terrain restricts approach by ground units.

A TUAV offers many advantages, including low cost, the ability to fly within a narrow space and the unique hovering and vertical take-off and landing (VTOL) flying characteristics.

The current state of TUAVs throughout the world is outlined [4]. A novel design of a multiple rotary wing platform which provide for greater SA in the urban terrain is then presented.

Autonomous vertical flight is a challenging but important task for TUAVs to achieve high level of autonomy under adverse conditions. The fundamental requirement for vertical flight is the knowledge of the height above the ground, and a properly designed controller to govern the process.

In [5], a three stage flight control procedure using three autonomous control subsystems for a nontrivial nonlinear

I. Astrov is with the Department of Computer Control, Tallinn University of Technology, Tallinn 19086, Estonia (phone: 372-620-2113, fax: 372-620-2101; e-mail: igor.astrov@dcc.ttu.ee).

A. Pedai is with the Department of Computer Control, Tallinn University of Technology, Tallinn 19086, Estonia (e-mail: andrus.pedai@dcc.ttu.ee).

B. Gordon is with the Department of Computer Control, Tallinn University of Technology, Tallinn 19086, Estonia (e-mail: boris.gordon@dcc.ttu.ee).

helicopter model on the basis of equations of vertical motion for the center of mass of helicopter was proposed. The proposed control strategy has been verified by simulation of hovering maneuvers using software package Simulink and demonstrated good performance for fast SA.

This paper concentrates on issues related to the area of [5], but demonstrates another field for application of these ideas, i.e., research technique using control system modeling and simulation on the basis of state-space equations of motion of coaxial unmanned helicopter with ducted fan configuration.

In this paper our research results in the study of vertical flight (take-off and hovering cases) control of unmanned helicopter with coaxial rotor and ducted fan configuration which make such SA task scenario as "go-search-find-return" possible are presented.

The contribution of the paper is twofold: to develop new schemes appropriate for SA enhancement using UAVs by hybrid control of vertical flight of unmanned helicopters, and to present the results of hovering maneuvers for chosen model of UAV for fast SA in simulation form using the MATLAB/Simulink environment.

II. UAV MODEL

In [6], a model of prototype coaxial unmanned helicopter with ducted fan configuration was proposed.

The prototype unmanned helicopter, with a net weight $160kg$ and height of $l=1.9m$, is a VTOL aircraft that includes a fuselage with toroidal portion and coaxial rotors. A duct is formed through the fuselage and extends from the top to the bottom of the fuselage. A propeller assembly is mounted to the top portion of the fuselage with a main rotor of diameter $4.4m$. A ducted rotor assembly is installed in fuselage compensating the propeller antitorque besides providing some fraction of lift. The coaxial rotors, main and ducted, rotate at $800rpm$ in opposite directions. The main rotor provides about 80% of lift, drag, pitch and roll movements of unmanned helicopter and the ducted rotor provides about 20% of lift and yaw movements.

In comparison with conventional main and tail rotor configuration, the coaxial rotors with ducted fan configuration provide more lift and move easily in any direction, during take-off and landing. These design features not only increase the maneuver ability of unmanned helicopter but also increase its stability making it easier to fly especially in narrow and bumpy take-off and landing site.

The dynamic model for control yields the general form of state equations for the prototype unmanned helicopter [6]

$$\dot{x}(\tau) = Ax(\tau) + Bu(\tau) + v(\tau) \quad (1)$$

$$y(\tau) = Cx(\tau) + w(\tau) \quad (2)$$

where $x(\tau), u(\tau), y(\tau), v(\tau), w(\tau)$ are the state, control input, output, process noise and measurement noise vectors, respectively.

The variables of this model are:

$$x = \begin{bmatrix} V_x \\ V_y \\ V_z \\ \omega_x \\ \omega_y \\ \omega_z \\ \phi \\ \theta \\ \psi \end{bmatrix}, u = \begin{bmatrix} \delta_{mr} \\ \delta_{lat} \\ \delta_{lon} \\ \delta_{fan} \end{bmatrix}, \quad (3)$$

where V_x, V_y, V_z are forward, lateral and vertical velocities; $\omega_x, \omega_y, \omega_z$ are roll, pitch and yaw rates; ϕ, θ, ψ are roll, pitch and yaw angles; $\delta_{mr}, \delta_{lat}, \delta_{lon}, \delta_{fan}$ are main rotor collective, lateral cyclic, longitudinal cyclic and fan collective pitches.

We notice that the velocities from (3) can be expressed in the form

$$V_x = \dot{x}_c, V_y = \dot{y}_c, V_z = \dot{z}_c \quad (4)$$

where x_c, y_c, z_c are coordinates of center of mass of UAV in the earth-frame.

Combining (3) and (4), we have

$$x = \begin{bmatrix} \dot{x}_c \\ \dot{y}_c \\ \dot{z}_c \\ \omega_x \\ \omega_y \\ \omega_z \\ \phi \\ \theta \\ \psi \end{bmatrix}, u = \begin{bmatrix} \delta_{mr} \\ \delta_{lat} \\ \delta_{lon} \\ \delta_{fan} \end{bmatrix} \quad (5)$$

The matrix structure of A, B, C for the state-space model of system (1)-(2) is given by

$$A = \begin{bmatrix} a_1 & a_2 & 0 & a_3 & a_4 & 0 & 0 & a_5 & 0 \\ a_6 & a_7 & 0 & a_8 & a_9 & 0 & a_{10} & 0 & 0 \\ 0 & 0 & a_{11} & 0 & 0 & a_{12} & 0 & 0 & 0 \\ a_{13} & a_{14} & 0 & a_{15} & a_{16} & 0 & 0 & 0 & 0 \\ a_{17} & a_{18} & 0 & a_{19} & a_{20} & 0 & 0 & 0 & 0 \\ 0 & 0 & a_{21} & 0 & 0 & a_{22} & 0 & 0 & 0 \\ 0 & 0 & 0 & 1 & 0 & 0 & 0 & 0 & 0 \\ 0 & 0 & 0 & 0 & 1 & 0 & 0 & 0 & 0 \\ 0 & 0 & 0 & 0 & 0 & 1 & 0 & 0 & 0 \end{bmatrix},$$

$$B = \begin{bmatrix} 0 & b_1 & b_2 & 0 \\ 0 & b_3 & b_4 & 0 \\ b_5 & 0 & 0 & b_6 \\ 0 & b_7 & b_8 & 0 \\ 0 & b_9 & b_{10} & 0 \\ b_{11} & 0 & 0 & b_{12} \\ 0 & 0 & 0 & 0 \\ 0 & 0 & 0 & 0 \\ 0 & 0 & 0 & 0 \end{bmatrix},$$

$$C = \begin{bmatrix} 1 & 0 & 0 & 0 & 0 & 0 & 0 & 0 & 0 \\ 0 & 1 & 0 & 0 & 0 & 0 & 0 & 0 & 0 \\ 0 & 0 & 1 & 0 & 0 & 0 & 0 & 0 & 0 \\ 0 & 0 & 0 & 1 & 0 & 0 & 0 & 0 & 0 \\ 0 & 0 & 0 & 0 & 1 & 0 & 0 & 0 & 0 \\ 0 & 0 & 0 & 0 & 0 & 1 & 0 & 0 & 0 \\ 0 & 0 & 0 & 0 & 0 & 0 & 1 & 0 & 0 \\ 0 & 0 & 0 & 0 & 0 & 0 & 0 & 1 & 0 \\ 0 & 0 & 0 & 0 & 0 & 0 & 0 & 0 & 1 \end{bmatrix}, \quad (6)$$

The parameters a_1 through a_{22} and parameters b_1 through b_{12} in (6) are given by:

$$\begin{aligned} a_1 &= 0.0058, \quad a_2 = 0.0017, \quad a_3 = 0.0081, \\ a_4 &= 0.0329, \quad a_5 = -9.8000, \quad a_6 = -0.0015, \\ a_7 &= -0.0058, \quad a_8 = -0.0329, \quad a_9 = 0.0081, \\ a_{10} &= 9.8000, \quad a_{11} = -0.9816, \quad a_{12} = 0.0794, \\ a_{13} &= -0.0072, \quad a_{14} = -0.0154, \quad a_{15} = -0.0867, \\ a_{16} &= 0.0153, \quad a_{17} = 0.0106, \quad a_{18} = -0.0049, \\ a_{19} &= -0.0106, \quad a_{20} = -0.0697, \quad a_{21} = -0.0416, \\ a_{22} &= -0.1691; \\ b_1 &= -0.1294, \quad b_2 = -2.8845, \quad b_3 = 2.8845, \\ b_4 &= -0.1294, \quad b_5 = 122.0518, \quad b_6 = 11.8688, \\ b_7 &= 7.5964, \quad b_8 = -0.9077, \quad b_9 = 0.8578, \\ b_{10} &= 7.2260, \quad b_{11} = -26.0034, \quad b_{12} = 10.7727. \end{aligned}$$

Then, we have

$$x_c(\tau) = \int_0^\tau \dot{x}_c(t) dt, \quad y_c(\tau) = \int_0^\tau \dot{y}_c(t) dt, \quad z_c(\tau) = \int_0^\tau \dot{z}_c(t) dt, \quad (7)$$

where

$$x_c(0) = 0, \quad y_c(0) = 0, \quad z_c(0) = 0.$$

From (1)-(2), (5)-(7) we can see that the attitude vector $(x_c, y_c, z_c)^T$ for given model of TUAV can be computed.

III. SIMULATION RESULTS

Consider the control of given TUAV model (1)-(2) with coaxial rotor and ducted fan configuration for the case of take-off and hovering maneuvers by hybrid constrained system of two control subsystems.

The goal of the following simulations is twofold. First, we verify that these control subsystems are able to control the take-off and hovering trajectories. Second, we observed the effect of enhancing SA because the variety of such trajectory parameter as main rotor collective pitch easily can be changed the possible take-off and hovering trajectories of given TUAV.

Initial and desired height for control subsystems are chosen to be:

$$x(0) = y(0) = z(0) = 0m, \quad z_1^0 = 20m, \quad z_2^0 = 49m.$$

Simulation results of the offered block scheme with two control subsystems (see Fig. 1) are shown in Figs. 4-8.

In [7], the two approximations to the nonlinear autoregressive moving average (NARMA) model called the NARMA-L1 and the NARMA-L2 are proposed. From a practical stand-point, the NARMA-L2 model is found to be simpler to realize than the NARMA-L1 model.

The neurocontrollers used in this section are based only on the NARMA-L2 approximate model [7].

Block diagram for the NARMA-L2 Controllers from Fig. 1 is given in Fig. 2. This controller can be implemented with the previously identified NARMA-L2 plant model, as shown in Fig. 3.

We simulated the block diagrams of subsystems as parts of hybrid control system and take into account that the full take-off and hovering trajectories were separated into initial and final phases with boundary point in the first lag position.

Fig. 4 shows the height trajectory of flight control.

Some advantages of this example are as follows.

- Opportunity of smooth switching of regulation from one neurocontroller to another.
- Possibility to consider a terrain restriction in a place of a hovering.
- Possibility of lag in two different selected height positions.
- Fine and simplified adjustment of these neurocontrollers for any changes of desired height positions.
- The trajectory tracking display forms give a researcher an immediate view of given TUAV motion with a range of such parameter as main rotor collective pitch. This allows us to investigate the sensitivity of the hybrid control system, providing a medium for such development and evaluation and enhancing the researcher's understanding of hovering maneuvers.

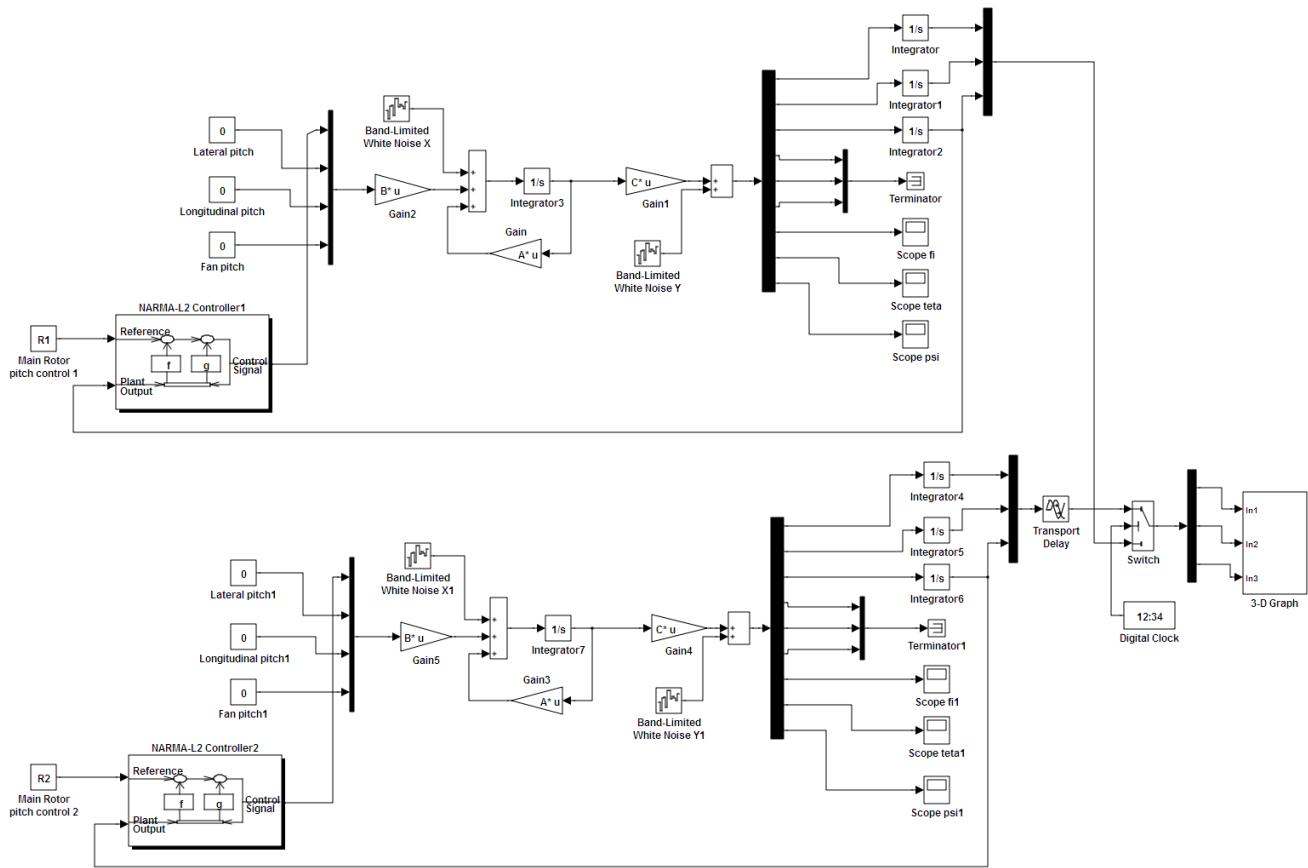


Fig. 1 Block diagram of hybrid control system

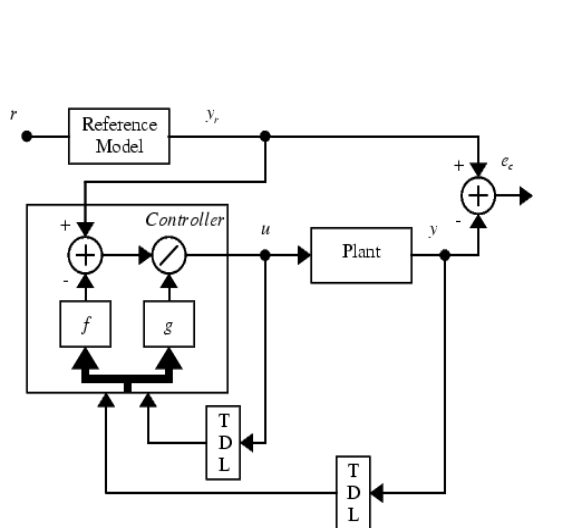


Fig. 2 Block diagram of the NARMA-L2 Controller

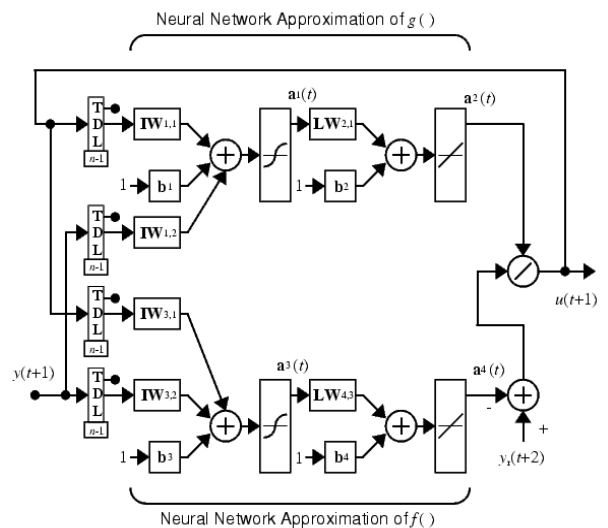


Fig. 3 Structure of a neural network representation for the NARMA-L2 approximate model

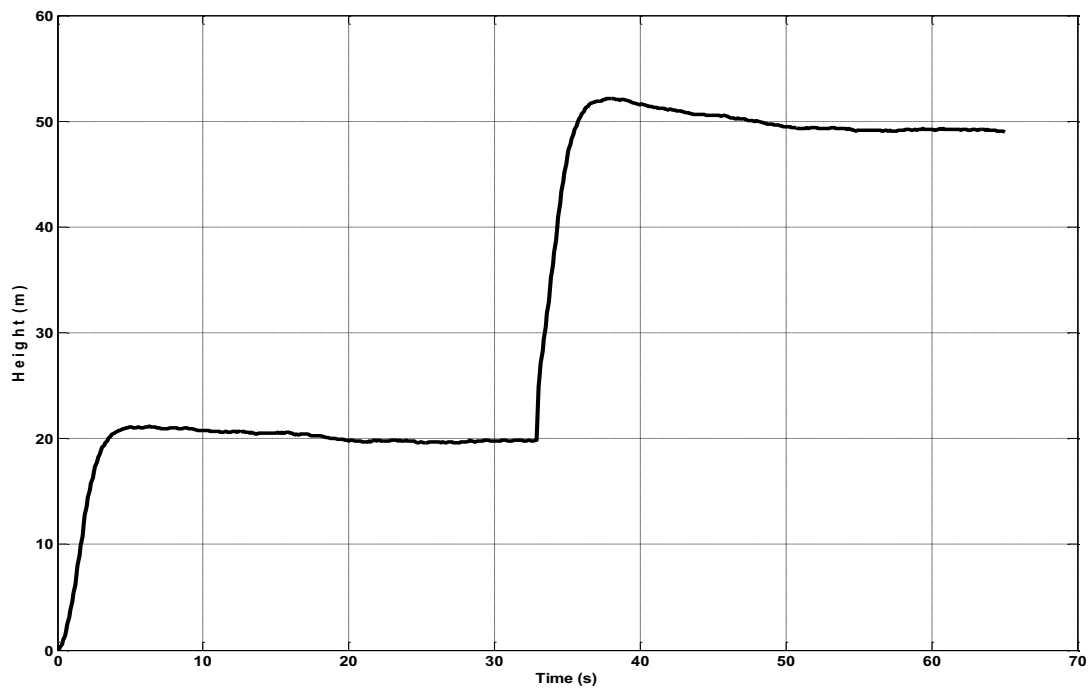


Fig. 4 Height trajectory of TUAV

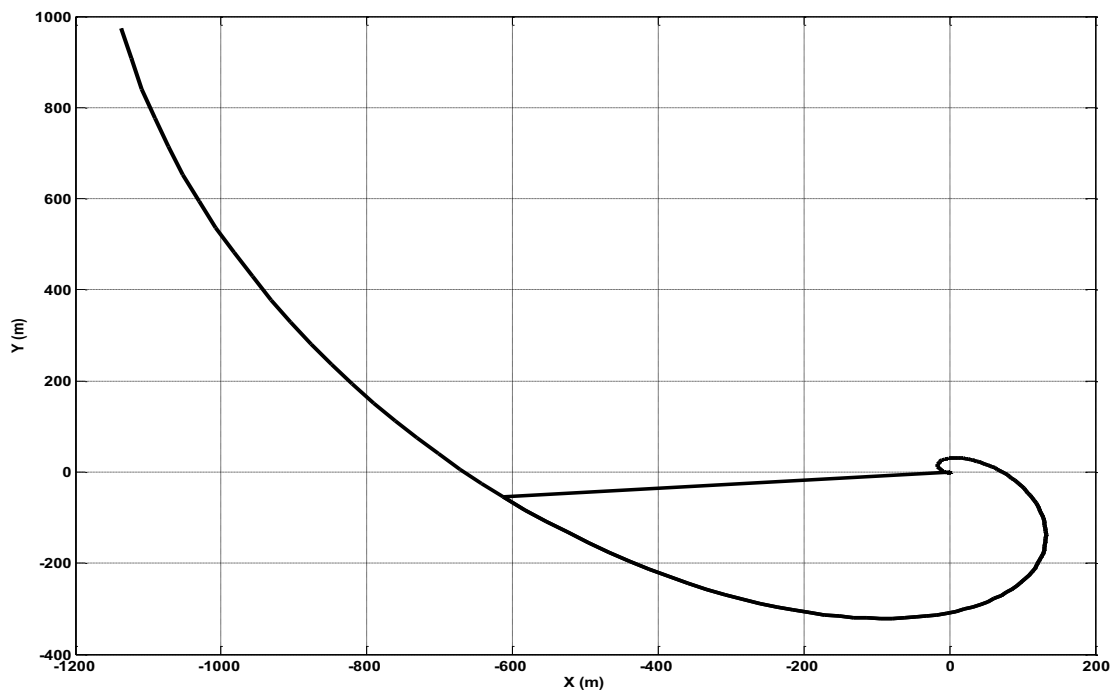


Fig. 5 X-Y view of TUAV's trajectory

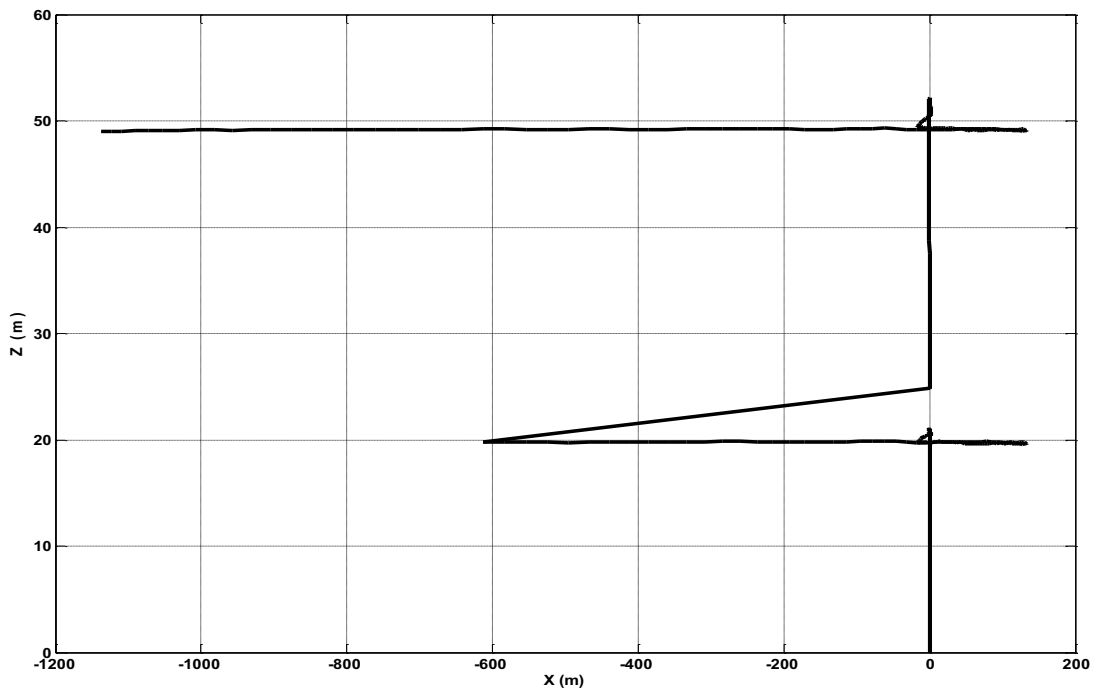


Fig. 6 X-Z view of TUAV's trajectory

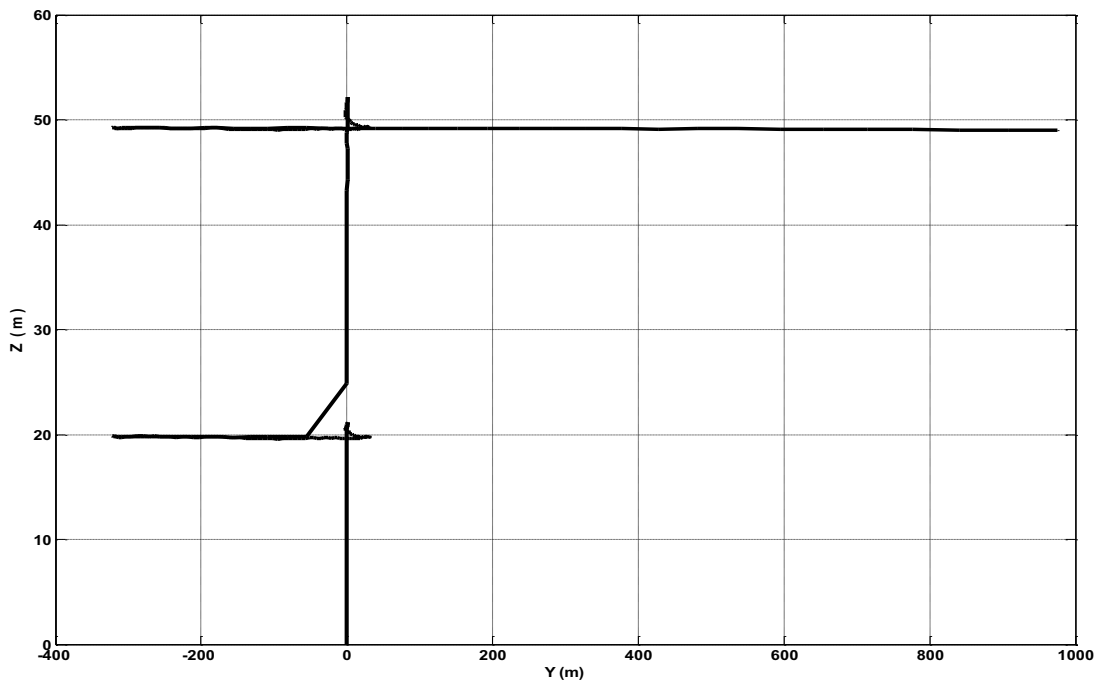


Fig. 7 Y-Z view of TUAV's trajectory

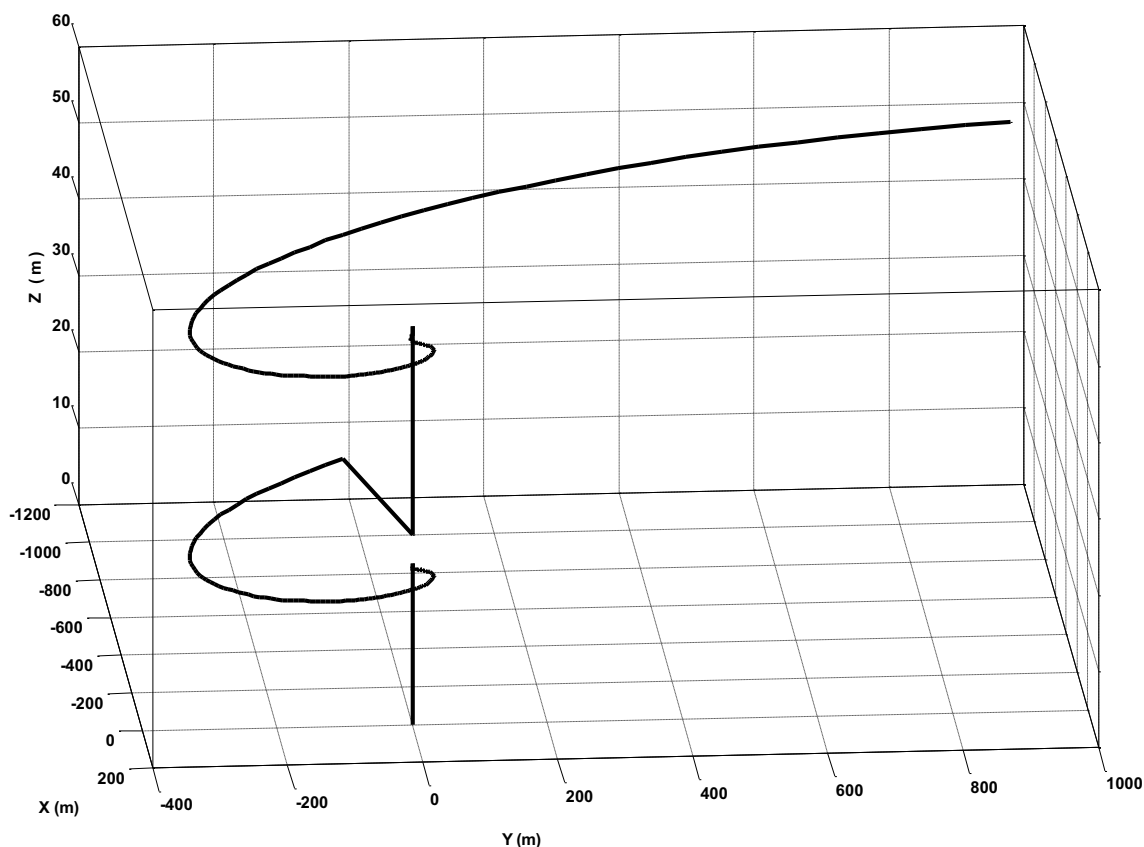


Fig. 8 3-D motion of TUAV

IV. CONCLUSIONS

A new research technique is presented in this paper for enhanced SA in possible missions of TUAV with coaxial rotor and ducted fan configuration.

The need for highly reliable and stable hovering for VTOL class TUAVs has increased morbidly for critical situations in real-time search-and-rescue operations for fast SA.

For fast, stable and smooth hovering maneuvers, we proposed a two stage flight strategy, which separates the flight process into initial and final phases. The effectiveness of the proposed flight strategy has been verified in field of flight simulation tests for chosen model of TUAV using software package Simulink.

From the applications viewpoint, we believe that this flight strategy furnishes a powerful approach for enhancing SA in applications to VTOL class autonomous vehicles.

Future work will involve further validation of the performance of the proposed research technique and exploring other relevant and interesting missions of TUAVs with coaxial rotor and ducted fan configuration.

REFERENCES

- [1] M. R. Endsley, "Toward a theory of situation awareness in dynamic systems," *Human Factors*, vol. 37, pp. 32-64, March 1995.
- [2] J. Gorman, N. Cooke, and J. Winner, "Measuring team situation awareness in decentralized command and control environments," *Ergonomics*, vol. 49, pp. 1312-1325, October 2006.
- [3] Interim Brigade Combat Team Newsletter. [Online]. Available: http://www.globalsecurity.org/military/library/report/call/call_01-18_toc.htm
- [4] S. D. Prior, S. T. Shen, A. S. White, S. Odedra, M. Karamanoglu, M. A. Erbil, and T. Foran, "Development of a novel platform for greater situational awareness in the urban military terrain," in *Proc. 8th International Conf. Engineering Psychology and Cognitive Ergonomics*, San Diego, USA, 2009, pp. 120-125.
- [5] I. Astrov and A. Pedai, "Control of hovering manoeuvres in unmanned helicopter for enhanced situational awareness," in *Proc. International Conf. Industrial Mechatronics and Automation*, Chengdu, China, 2009, pp. 143-146.
- [6] S. Shouzhao, A. A. Mian, Z. Chao, and J. Bin, "Autonomous takeoff and landing control for a prototype unmanned helicopter," *Control Engineering Practice*, vol. 18, pp. 1053-1059, September 2010.
- [7] K. S. Narendra and S. Mukhopadhyay, "Adaptive control using neural networks and approximate models," *IEEE Trans. Neural Networks*, vol. 8, pp. 475-485, May 1997.